Review

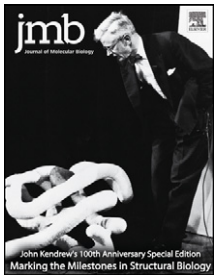

Structural and Molecular Biology of a Protein-Polymerizing Nanomachine for Pilus Biogenesis

Gabriel Waksman

Institute of Structural and Molecular Biology, *Birkbeck College, Malet Street, London WC1E 7HX, UK*
Institute of Structural and Molecular Biology, *University College London, Gower Street, London WC1E 6BT, UK*

Correspondence to Gabriel Waksman: *g.waksman@mail.cryst.bbk.ac.uk*
http://dx.doi.org/10.1016/j.jmb.2017.05.016
Edited by I B. Holland

Abstract

Bacteria produce protein polymers on their surface called pili or fimbriae that serve either as attachment devices or as conduits for secreted substrates. This review will focus on the chaperone–usher pathway of pilus biogenesis, a widespread assembly line for pilus production at the surface of Gram-negative bacteria and the archetypical protein-polymerizing nanomachine. Comparison with other nanomachines polymerizing other types of biological units, such as nucleotides during DNA replication, provides some unifying principles as to how multidomain proteins assemble biological polymers.

Introduction

Pili (or fimbriae) are widespread protein polymers that form organelles at the surface of Gram-negative and -positive bacteria and archaea. In Gram-negative bacteria, depending on their assembly mechanisms, they can be categorized into five different classes: (i) chaperone–usher (CU) pili, (ii) curli, (iii) type IV pili, (iv) type V pili, and (v) type IV secretion pili [1]. Pili of the first four classes are mostly used for adhesion, host recognition, and/or biofilm formation, while pili of the fifth class may be used as a conduit for secretion of effector proteins or single-stranded DNAs [2–5]. All five categories have defined structures and defined mechanisms of assemblies mediated by distinct and sometimes extremely elaborated pilus biogenesis mechanisms: the machineries responsible for producing type IV pili and type IV secretion pili are very large, composed of tens of components assembling in various stoichiometries to form multimegadalton complexes in size embedded in both the inner and outer membranes [1,6,7]; those producing CU pili and curli are much simpler both in composition and size and are located at the outer membrane [8–11]. As a consequence of their location, while the double-membrane-embedded nanomachines are able to use ATP from the cytoplasm, the outer-membrane-embedded systems cannot, as there is no ATP in the periplasm, the compartment between the inner and outer membranes. Thus, these systems must energize the assembly process in different ways.

Investigations of pilus-producing machineries have provided mechanistic details, but none has yet yielded as much information as those that have focused on the CU pathway of pilus biogenesis. This is because this system has proved more amenable than most to structural, biochemical, and biophysical characterization. In this review, I describe how successive breakthroughs have led to detailed mechanistic insights on this relatively simple molecular machine capable of polymerizing protein subunits and secreting the resulting polymer.

Type P and 1 Pili

Type P and 1 pili have served as model systems for CU pili. These filaments are elaborated by strains of *Escherichia coli* able to infect the urinary tract of higher eukaryotic hosts including humans. They play important roles in the process of infecting the host bladder and kidney by mediating attachment of the bacterium to these organs' epithelia [12–14].

P pili are elaborated from six types of subunits encoded by the *pap* cluster in *E. coli*. In a P pilus,

these subunits appear in a defined order, starting at the tip with the PapG subunit, a protein termed "adhesin", which binds Galα-1,4-Galβ receptors lining the kidney epithelium, followed successively by one copy of the PapF subunit, 5–10 copies of the PapE subunit, 1 copy of the PapK subunit, circa 1000 copies of the PapA subunit, and finally 1 copy of PapH at the pilus base. PapG to PapK forms a rather short, flexible part termed "the tip fibrillum", while the numerous PapA subunits form a helically wound polymer of 3.3 subunits per turn, termed a "rod" and forming most of the 2-μm pilus [3,15–19] (Fig. 1). A type 1 pilus is composed of four subunits encoded by the *fim* cluster in *E. coli*. Its tip fibrillum is shorter than that of P pili, being composed of one copy each of only three subunits, the adhesin FimH at the tip, followed by the FimG subunit, and the FimF subunit. Its rod is similar to that of P pili, containing circa 1000 subunits of FimA, also helically wound with a similar number of subunits per turn [3,15,16] (Fig. 1). FimH binds D-mannosylated receptors, such as uroplakins, found on the surface of the bladder epithelium [20,21]. Thus, while P pili are thought to mediate the attachment of uropathogenic *E. coli* to the kidney to cause pyelonephritis, type 1 pili mediate the attachment of bacteria to the bladder to cause cystitis.

All pilus subunits, except the tip adhesins, fold into a single domain termed "pilin" domain that serves as "lego" block for assembly [22,23]. The tip adhesins are the exception as they are composed of two domains, an N-terminal "adhesin" domain, which mediates receptor interaction, and a C-terminal pilin domain that is used as lego block for assembly [23,24]. While adhesins usually exhibit unremarkable lectin folds, pilin domains have a singular structure consisting of a C-terminally truncated Ig fold: regular Ig folds include seven strands, A to G, folding into a common β-sandwich; however, pilus subunits lack strand G [22,23] (Fig. 2).

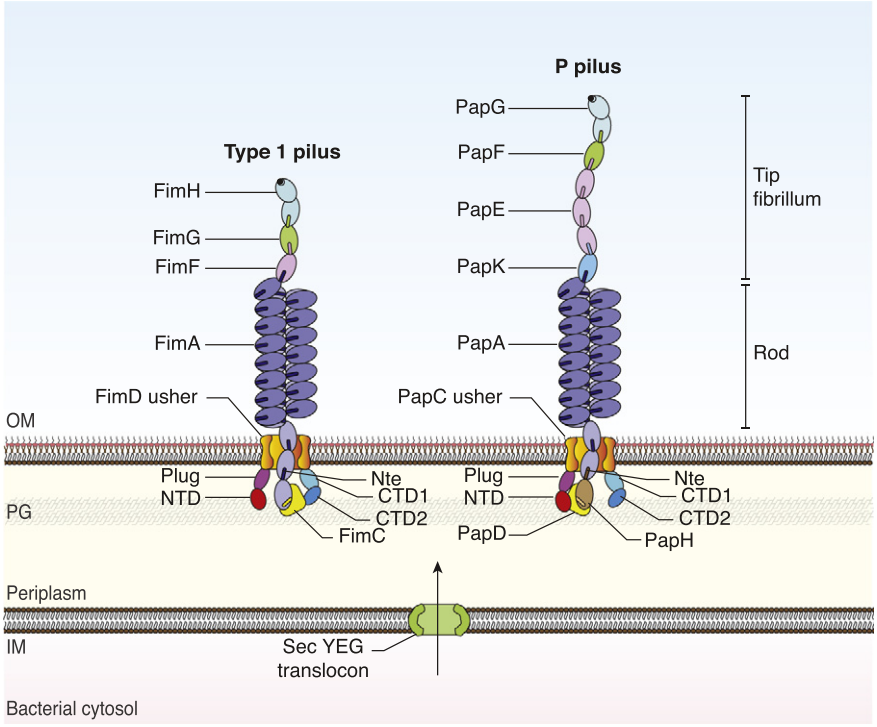

Fig. 1. Schematic diagram of P and type 1 pili. A schematic diagram of a type 1 and a P pilus is shown. Subunits and usher domains in each system are labeled and color-coded differently. This color-coding is used consistently throughout the review. The black dot at the tip of FimH and PapG indicates the receptor-binding site. P and type 1 pili are archetypal pili composed of six (PapG, F, E, K, A, and H) and four (FimH, G, F, and A) known subunits, respectively, assembling in a defined order. Each subunit traverses the inner membrane using the SecYEG translocon, at the exit of which the subunit is received by the periplasmic chaperone PapD or FimC for P and type 1 pili, respectively. The chaperone assists in subunit folding by donating one of its own strands to the C-terminally truncated Ig fold of the subunit to form stable binary chaperone–subunit complexes. These complexes are then ferried for assembly to the usher, an outer membrane protein composed of five domains, NTD, plug, pore, CTD1, and CTD2. The usher orchestrates subunit polymerization by catalyzing the substitution of the chaperone strand by the N-terminal sequence (or Nte) of the subunit next in assembly (Ntes are indicated here in short thick dashes).

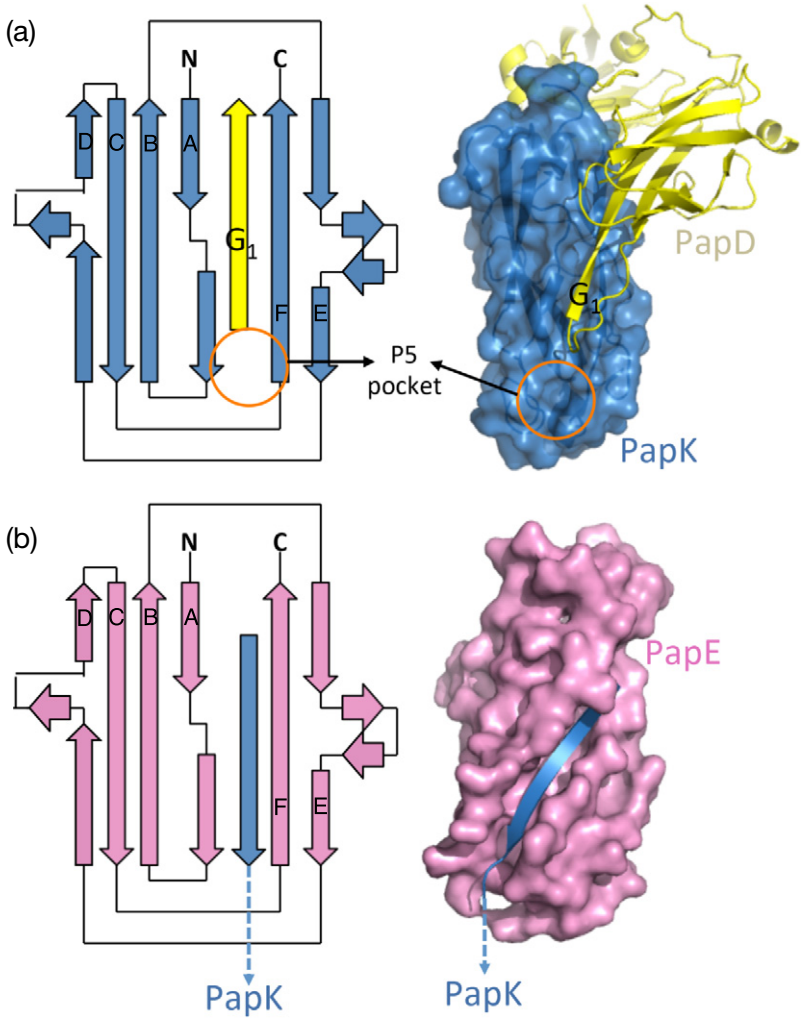

Fig. 2. Donor-strand complementation (DSC) and donor-strand exchange (DSE). In both panels, a topology diagram is shown at the left, while the structure is shown at the right. In the topology diagram, β-stands are shown as arrows and are labeled. In the structure, the subunit is shown in surface representation, while the (a) chaperone or (b) subunit providing the complementing strand are shown in cartoon representation. (a) DSC. CU chaperones stabilize CU pilus subunit via DSC. Pilus subunits (in blue) are Ig-folded proteins lacking strand G, the Ig fold's C-terminal strand. The chaperone (in yellow) assists in folding the subunit and stabilizes it by providing *in trans* one of its own strand, strand G_1. Here, the PapD–PapK complex is shown (PDB entry code 1PDK). Also shown in a red circle is the location of the P5 pocket where the P5 residue of the next subunit's Nte inserts to initiate DSE. (b) DSE. During DSE, strand G_1 of the chaperone is replaced by the Nte of the subunit next in assembly. DSE proceeds via a zip-in-zip-out mechanism starting with the insertion of the P5 residue of the subunit's Nte next in assembly into the P5 pocket of the subunit. Here, the complex of PapE (in light magenta) bound to the Nte of PapK (in blue) is shown (PDB entry code 1N12).

Chaperone-Assisted Folding of Pilus Subunits—Donor-Strand Complementation

Because they lack a strand at their C terminus, pilus subunits cannot fold by themselves and thus require a chaperone that not only assists in folding but also provides *in trans* the secondary structure missing in pilus subunits [25,26] (Fig. 2).

The chaperones PapD and FimC operate in the assembly of P and type 1 pili, respectively. These chaperones have very similar structure, displaying two consecutive Ig-folded domains, termed “domain 1” and “domain 2”, which make a 45° angle relative to one another, lending to the protein the shape of a boomerang [27]. Both PapD and FimC are able to catalyze subunit folding *in vitro* in a mechanism that still remains to be characterized fully but that is thought to be seeded by the interactions of the subunit's terminal carboxylate with two basic residues at the angle between the two handles/domains of the boomerang-shaped chaperone and also possibly by the zippering of the subunit's C-terminal strand, strand F, along the G strand of the chaperone's domain 1 (termed the “G1 strand”) [25,26,28].

The importance of the chaperone's G1 strand in stabilizing the subunit was revealed by structures of the first chaperone-subunit complexes ever determined, PapD–PapK and FimC–FimH [22,23] (Fig. 2). Because of the lack of a C-terminal strand, a distinctly deep groove is observed at the surface of the subunit, where the C-terminal strand should be. This groove is hydrophobic, as the hydrophobic core of the protein is exposed due to the missing strand. This groove can be subdivided into five sites/pockets termed “P1 to P5 pockets”. In both complexes, the G1 strand of the chaperone was found inserted between strands F and A2 of the Ig-folded subunit, filling the subunit's groove. More specifically, four primarily hydrophobic and alternating, residues, termed “P1 to P4 residues”, in the chaperone's G1 strand interact with the subunit groove's P1 to P4 pockets, leaving the P5 pocket free (Fig. 2). Thus, the chaperone folds and stabilizes

subunits by donating *in trans* one of its own strands, G1, thereby providing the subunits with its full complement of strands. However, the subunit's Ig fold reconstituted by the donation of the chaperone's strand is non-canonical, as the donated strand runs parallel to strand F, not antiparallel as strand G would in a canonical Ig fold. This unusual topological arrangement of secondary structures maintains subunits in a metastable state, a state that "primes" subunit for reaction with other subunits during polymerization (see below).

In vivo, chaperone-assisted folding of pilus subunits occurs in the periplasm, the space between the inner and outer membranes of Gram-negative bacteria. Pilus subunits contain N-terminal signal sequences that target them to the SecYEG translocon for transport through the inner membrane. When emerging from the translocon on the periplasmic side, pilus subunits interact with their cognate chaperone, presumably initiating folding and complex formation in a mechanism similar to that described *in vitro* (see above). This would require PapD or FimC to be pre-positioned favorably to receive the subunit's terminal carboxylate and operate F strand zippering along the chaperone's G1 strand as the subunit emerges from the SecYEG translocation gate. Unfortunately, the positioning of PapD or FimC onto the periplasm-facing surfaces of SecYEG is not known, and thus, it is unclear how folding *in vivo* might occur.

Polymerization of Pilus Subunits—Donor-Strand Exchange

The chaperone is never part of the pilus, and thus, at some point during pilus biogenesis, the chaperone must dissociate and its G1 strand must be replaced by a structural element from the subunit next in assembly. Sequence conservation was observed in the N-terminal sequences of pilus subunits, and truncations of these sequences were shown to abrogate polymerisaton of subunits *in vitro*, suggesting that the N terminus of each subunit plays a role in polymerization [29].

Each subunit indeed contains a 10- to 20-residue sequence at its N terminus, termed "N-terminal extension (Nte)", characterized by a motif of alternating hydrophobic residues and a strictly conserved Gly residue [22,29]. Peptides derived from Ntes are able, on their own, to challenge ("attack") chaperone–subunit complexes, trigger chaperone dissociation, and form a complex with the challenged subunit [30,31]. Structures of such complexes revealed that the attacking Nte peptide has replaced the chaperone G1 strand in the groove of the challenged subunit [30–32] (Fig. 2). The peptide fills in the groove with at least four (as in the case of PapE, for example) or sometimes all five (as in the case of PapA) groove's pockets interacting with the Nte's alternating hydrophobic motif residues, which we termed "P1 to P5 residues", as they occupy either the P2 to P5 (PapE) or P1 to P5 (PapA) pockets of the groove in which they insert. Importantly, the Nte peptide runs antiparallel to strand F of the challenged subunit, thereby reconstituting a canonical Ig fold for the challenged subunit. The same overall structural features were observed when full-length subunits were observed bound to other full-length subunits [8,9,32–34]. Thus, during polymerization, subunits undergo a topological transition from a non-canonical Ig-folded structure, where the seventh strand parallel to strand F is provided by the chaperone, to a canonical Ig-folded structure where the seventh strand, this time antiparallel to strand F, is provided by the Nte of the subunit next in assembly. This topological transition is coupled to a structural transition from a metastable state to a tight state, respectively, where the subunit adopts a much tighter structure and where the topologically canonical conformation results in one of the tightest non-covalent interaction known in nature [30,35,36]. The process whereby the strand donated by the chaperone is replaced by the Nte of the subunit next in assembly is termed "donor-strand exchange (DSE)" [30].

Determinants of the DSE Reaction—Role of the P5 Pocket

The observations that in the chaperone–subunit complex, the P5 pocket is free while it is occupied in the subunit–Nte complex and that a topological transition is observed between the two complexes with the strand donated by the chaperone running in opposite direction to the strand donated by the subunit next in assembly suggested a potential zip-in-zip-out mechanism for DSE initiated by the insertion of the attacking Nte's P5 residue within the challenged subunit groove's P5 pocket [31]. Indeed, a transient ternary complex between an attacking Nte and a chaperone–subunit complex was observed by mass spectrometry [31]. The formation of this ternary complex is crucially dependent on the Nte's P5 residue. Thus, DSE starts with the insertion of the attacking Nte's P5 residue into the challenged subunit groove's P5 pocket, thereby positioning the Nte ideally for invasion of the groove and progressive replacement of the chaperone strand within it [37]. This mechanism for DSE was termed "zip-in-zip-out" to illustrate the fact that the zipping in of the Nte within the challenged subunit's groove occurs concomitantly to the zipping out of the chaperone's G1 strand.

DSE may occur spontaneously when a chaperone–subunit complex is challenged by a peptide derived from subunit's Ntes, but the rate at which the reaction takes place varies enormously depending on the Nte *versus* chaperone–subunit pair, from being very fast when the Nte used in the reaction is that of the subunit

known to be assembled after the subunit being challenged (such a pair is termed "cognate") to being extremely slow when this is not the case ("non-cognate") [38]. In a study exploring systematically all Nte *versus* chaperone–subunit pairs in the P pilus system, it was shown, for example, that the PapD–PapG complex undergoes fast DSE with the Nte of PapF, but not with the Nte of any other Pap subunit, explaining why PapF is next in assembly after PapG [38]. More generally, whether in the absence of the usher or in its presence, it has been shown that DSE reactions are fastest between cognate pairs of subunits [38]. Thus, a suitable steric fit between Ntes and subunit's grooves is important in mediating subunit ordering within the pilus. Strikingly, within Ntes, residues at and around the P5 residue were shown to be the main determinants of the DSE reaction between cognate pairs: thus, specificity of subunit–subunit ordering is not only mediated by Nte–groove interaction but also more importantly driven kinetically by the initial P5 pocket–P5 residue interaction prior to groove invasion [39].

The crucial role that the interaction between the P5 residue and the P5 pocket plays in orchestrating DSE was put into sharp focus by the observation that the termination subunit PapH is the only Pap subunit that does not have a P5 pocket. CU pilus length is not strictly fixed; rather, it is characterized by a sharp Gaussian distribution around a mean of about 2 μm. This mean value is shifted toward shorter lengths when PapH is overexpressed; conversely pili are very long and detached when the *papH* gene is knocked out. Thus, pilus biogenesis termination is dictated by the incorporation of PapH in a stochastic manner dependent on PapH concentration: the higher the PapH subunit concentration is within the periplasm, the shorter the mean length of pili per bacteria. Remarkably, PapD–PapH complexes are remarkably stable, being the only chaperone–subunit complexes in the Pap system that cannot be disrupted by any Nte sequences or any other peptides [40]. This remarkable inability of PapH to undergo DSE is uniquely due to a lack of P5 pocket; thus, no Nte can interact with PapH to form the transient ternary complex state necessary to initiate PapH groove invasion [40]. No termination subunit has yet been identified in the type 1 pilus system, and thus, it is still unclear how pilus biogenesis in this system might occur.

The Usher—A Catalyst of DSE

The usher is a large outer membrane protein that orchestrates the polymerization and secretion of the pilus *in vivo* [41,42]. Polymerization of pilus subunits can occur in the absence of the usher, but reaction rates are slow, in the order of hours, and, in the case of PapA, leads to the formation of rods, which, compared to the rods produced *in vivo*, may be 10 times shorter [33,38]. The usher greatly increases the rate at which pili are produced, in the order of a few minutes, and thus can be considered a catalyst of the DSE reaction [43,44].

To carry out its function, the usher must be able to recruit chaperone–subunit complexes, execute the DSE reaction between subunits, and secrete the nascent pilus through its pore. Fortunately, thanks to the rewarding willingness of the usher to yield to the best efforts of structural biologists and biochemists, most aspects of its mechanistic underpinnings have been elucidated.

The usher consists of five domains, each endowed with a specific role in usher function (Fig. 3). The first 125 residues form an N-terminal domain (NTD) responsible for chaperone–subunit complex recruitment. It is followed by ~500 residues forming a 24-stranded β-barrel pore, the sequence of which is interrupted by a 90-residue plug domain that obstructs the β-barrel pore in the resting state of the usher, thereby sealing the pore when the usher is not engaged. Finally, there are two C-terminal domains, CTD1 and CTD2, which form a secondary chaperone–subunit binding platform [8].

The usher NTD is the primary binding site for chaperone–subunit complexes. This is where these complexes are recruited first. Chaperone–subunit complexes have various affinities for the usher NTD, with the chaperone–adhesin complex (the subunit at the tip of the pilus) exhibiting the highest affinity among all complexes, explaining in part why the chaperone–adhesin complex is recruited first and therefore its position at the tip of the pilus [45–49]. However, affinities between usher NTD and all other chaperone–subunit complexes do not correlate with their order of assembly; order of assembly correlates much better with the DSE kinetics of cognate/non-cognate Nte–subunit pairs (see above). Overall, except for the chaperone–adhesin complex, affinities for the usher NTD are rather weak in the order of 10–20 μM. As in all attempts to rationalize molecular interactions, it is difficult to model accurately how affinity relates to binding site occupancy without a knowledge of concentration; however, given the confined environment of the periplasmic compartment, it is expected that the local concentration of chaperone–subunit complexes around the usher may be high, and thus, in spite of apparently low affinities, the usher NTD might be reasonably highly occupied. Interestingly, the plug domain, which in the engaged state of the usher locates next to the NTD, appears to also play a role in the binding of chaperone–subunit complexes, extending the binding surface area of the NTD [49].

The translocation domain forms a pore through which the nascent pilus passes. This was demonstrated by the structure of the FimD usher (the usher for the type 1 pilus system) bound to its cognate chaperone–adhesin complex, FimC:FimH, where the lectin domain of the FimH subunit is observed inside the FimD pore

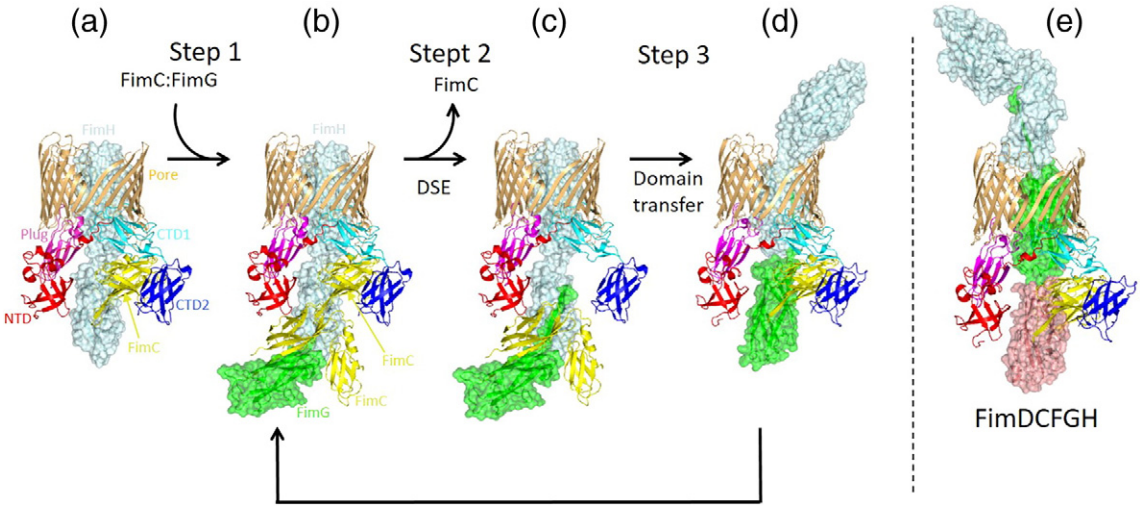

Fig. 3. Subunit incorporation cycle by the FimD usher. Color-coding of chaperone–subunit complexes and domain ushers is as in Fig. 1. (a) The cycle of subunit incorporation starts with the formation of the FimD–FimC–FimH complex (PDB entry core 3RFZ). In this crystal structure, FimC:FimH is bound to the chaperone–subunit complex binding site formed by the usher CTDs. (b) The usher NTD is available for binding. In the first step of the cycle (step 1), the next chaperone–subunit (FimC–FimG) in assembly is recruited in the usher NTD [this structure is a hypothetical model that was obtained by superposing 3RFZ (crystal structure of full-length FimD:FimC:FimH) and 3BWU (crystal structure of the FimD NTD bound to a chaperone–subunit complex)]. In this complex, the P5 residue of the FimG Nte locates above the P5 pocket of FimH, in an ideal configuration for the DSE zip-in-zip-out process between the two subunits to proceed (step 2). (c) During this process, the chaperone bound to FimH and the CTDs dissociates, resulting in the chaperone–subunit binding site formed by the CTDs being vacated [this structure is a hypothetical model that was obtained by using the structure shown in panel (b) and by modeling the Nte of FimG bound to the groove of FImH as in the crystal structure of the FimD–FimC–FimH–FImG–FImF complex (PDB entry code 4J30)]. (d) In the last step of the subunit incorporation cycle (step 3), FimC–FimG transfers to the CTDs (this structure is a hypothetical model that is, however, virtually identical to the crystal structure of full-length FimD–FimC–FimH or FimD–FimC–FimH–FimG–FimF, except that only two subunits are shown here, FimH and FimG). This transfer consists of a rotation of about 110° and a translation of about 50 Å, resulting in the translocation of the nascent pilus within the pore and in the usher NTD free to bind the next subunit in assembly (step 1). The crystal structure of the FimD:FimC:FimH:FimG:FimF is shown in panel (e).

[8]. In the resting state of the usher, the pore is occluded by the plug domain, but in a process still poorly understood, the plug can disengage and swing out to let FimH through [50]. Only recruitment of the chaperone–adhesin complex can trigger this process of usher activation; no other chaperone–subunit complex can [42,43,51]. A plausible mechanism of usher activation is suggested by two observations: (i) electrophysiological recording of current passing through ushers embedded in artificial bilayers exhibits very rapid bursts of current, indicating that the plug may intermittently and very rapidly swing out [52]; and (ii) the "swing out" state of the plug appears to be stabilized by interactions with chaperone–subunit complexes [8]. Thus, binding of the chaperone–adhesin complex to the usher NTD may form a preinitiation complex whereby the adhesin complex "lurks" in wait for the plug to come out and then engages its lectin domain inside the pore once the plug is out. The "out" state of the plug would be stabilized by the chaperone–adhesin complex itself, therefore providing a window of opportunity for the adhesin to engage the pore. Alternatively, binding of the chaperone–adhesin complex may trigger a conformational change in the pore itself, leading to the expulsion of the plug. It is, however, unclear how this might happen, and thus, at this moment in time, spurious opening event as seen in the current recording experiment appears the most plausible mechanism.

In the complex of the FimD usher bound to the chaperone-adhesin complex FimC:FimH (Fig. 3), the chaperone–adhesin complex is observed bound to the CTDs. Thus, after recruitment to the NTD and once engaged in the pore through its adhesin domain, the chaperone–adhesin complex transfers to the CTDs. Mechanistically, there are two pieces of evidence that might provide a basis on which this transfer mechanism might be understood. Firstly, the FimD CTDs provide a high-affinity substrate binding site [70] with the usher CTD2 alone able to compete off chaperone–subunit complexes bound to the NTD [49]. These experiments were carried out in solution with purified proteins, and thus, it is envisageable that this competitive binding reaction would be even more favored (due to increased local concentration) when the NTD and CTDs are within proximity in the full-length usher at the membrane. Secondly, a computational study examining the interactions that

subunits make within the usher pore has revealed a helical free-energy pathway within the usher pore [9]. This helical pathway would impose a rotation of about 2–2.5° per Å translation, which, over the length of the pore (about 50 Å), would result in the ~110° rotation of the subunit engaged within it. Thus, while the pilus is being extruded from the usher pore, it would undergo a rotation, the extent of which is exactly what would be necessary to bring the chaperone–subunit complex at the base of the nascent pilus from the NTD to the CTDs.

A Model for the Subunit Incorporation Cycle by the Usher

Most machines involved in polymerization of biological units incorporate functional units through incorporation cycles one unit at a time. All require an initiation step, a multitude of elongation steps and a termination step. All cycle through conformational changes, the series of which repeat itself until a termination signal is encountered. A particularly well-studied example of such a nanomachine is DNA polymerase I (DNA Pol I), responsible for template-directed DNA replication. This enzyme cycles through a number of conformational changes in order to extend a primer strand by 1 nucleotide [53,54]. This nucleotide incorporation cycle was first described kinetically and, later on, structurally in great details. The usher also cycles through a series of conformational changes in order to add one subunit to a nascent pilus, and some of the principles established for the nucleotide incorporation cycle by DNA Pol I enzymes also apply to the subunit incorporation cycle by the usher.

One interesting parallel is the way both the usher and DNA Pol I utilize different parts of their structure for distinct purposes during the cycle. The best structurally characterized DNA Pol I enzyme is the Klenow fragment of *Thermus aquaticus* DNA Pol I, termed "Klentaq1" [55–57]. Klentaq1 consists of two domains, an NTD deprived of any function and a large CTD, which contains the polymerase activity [55]. This polymerase domain is itself subdivided into three subdomains that play distinct roles during the nucleotide incorporation cycle (Fig. 4). The "Thumb" subdomain is primarily responsible for clamping the primer–template DNA in place [56]; the "Palm" subdomain contains the active side residues and thus is responsible for the reaction between the 3′ OH end of the primer and the nucleoside triphosphate (dNTP) [56]; the "Fingers" subdomain is responsible for recruiting dNTPs and delivering them to the active site [56,57]. In brief, there are two forms of Klentaq1 [56]. The first form is an open form where the Fingers subdomain is in an open position and where the dNTP-binding site is exposed, and thus, dNTP can bind; in this open conformation, the dNTP bound to the dNTP-binding site is too far from the active site, and therefore, the polymerization reaction cannot occur. The second form is a closed form where the Fingers subdomain undergoes a 46° inward rotation toward the Palm subdomain, bringing the bound dNTP to the active site, to form a reaction-competent complex that leads to nucleotide addition to the primer's 3′ end. Thus, the nucleotide incorporation cycle proceeds in the following manner (Fig. 4). The cycle starts with the primer–template DNA binding to the enzyme. This binding event is accompanied by a conformational change in the Thumb subdomain that wraps around the DNA to clamp it in place. At this stage, the Fingers subdomain is constantly transitioning (or flapping) between its open and closed form (as shown by single-molecule Fluorescence resonance energy transfer (FRET) measurements [58]). When it is in its open form, it is available for binding dNTP, which, through the flapping motion, is brought to the active site. There, the base of the incoming dNTP is evaluated for its Watson–Crick pairing with the base of the template DNA against which the incoming nucleotide base aligns [59]; if the Watson–Crick pairing is correct, the enzyme locks in the closed form, active site residues position themselves around the dNTP, two $Mg2+$ ions, water molecules, and the 3′ OH of the primer strand, and the reaction occurs linking the primer's 3′OH with the 5′ α-phosphate of the dNTP. The reaction is followed by the release of the Fingers subdomain to the open position and the translocation of the primer–template DNA. At this stage, a new nucleotide incorporation cycle can start.

While the initiation step for the nucleotide incorporation cycle is the loading of the polymerase on the primer–template DNA and the clamping of the thumb domain onto the DNA, that of the subunit incorporation cycle by the usher is the loading of the chaperone–adhesin complex (see details above). After this, the elongation cycle in both nanomachines, DNA Pol I and the usher, strikingly, follows some of the same principles. In the usher (Fig. 3), the first step in the subunit, incorporation cycle is the recruitment of the next chaperone–subunit complex in assembly (FimG in the type 1 pilus) by the usher NTD. As mentioned above, affinities for chaperone–subunit other than chaperone–adhesin complexes are low, and thus, presumably, the usher NTD might be occupied intermittently by chaperone–subunit complexes other than FimC:FimG. However, crucially, when bound to the usher NTD, the chaperone–subunit complex is positioned relative to the previously assembled chaperone–subunit complex (here FimC:FimH) in such a way that the P5 residue of its Nte locates right above the P5 pocket of the FimH groove, in an ideally "catalytic" configuration for DSE. As pointed out previously, the P5 residue–P5 pocket interaction is the primary determinant of subunit ordering, and therefore, DSE can only proceed if the right steric fit between the two is achieved. Thus,

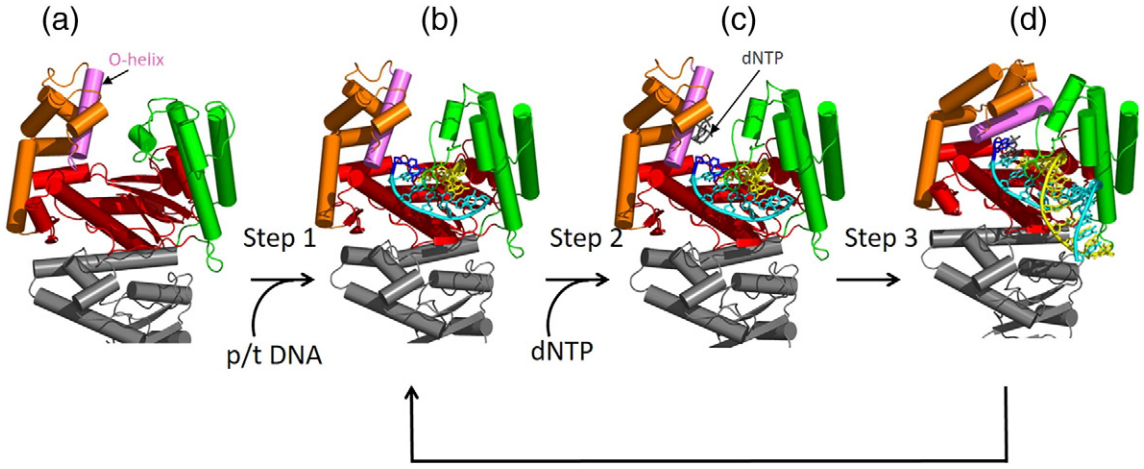

Fig. 4. Nucleotide incorporation cycle by the Klentaq1 DNA Pol I enzyme. The panels zoom in on the polymerase domain, but the vestigial 3′–5′ exonuclease domain is also partly shown in gray. The polymerase domain is color-coded by subdomains using the following keys: the Thumb subdomain in green, the Palm subdomain in red, and the Fingers subdomain in orange, except for the O-helix in the Fingers subdomain that is shown in light magenta. The O-helix contains the dNTP-binding site, to which dNTPs are recruited. The primer–template (p/t) DNA is shown in yellow and cyan, respectively, except for the templating base in the template strand that is shown in blue. The templating base is so-called because it is the first unpaired base of the template strand. It is also the base against which the incoming nucleotide (the one next in assembly) will align and evaluate its Watson–Crick pairing. The incoming nucleotide is shown in dark gray. The nucleotide incorporation cycle starts with the binding of the primer–template (p/t) DNA (step 1). The apo (PDB entry code 1KTQ) and p/t-bound (PDB entry code 2KTQ) forms are shown in panels (a and b), respectively. The binding of the p/t DNA is accompanied by a conformational change at the tip of the Thumb subdomain, resulting in the Thumb and Palm subdomains almost completely surrounding the p/t DNA. (c) In step 2, the dNTP is recruited to the O-helix at the tip of the Fingers subdomain [this structure is a hypothetical model that was obtained by superposing the structures of the p/t DNA-bound and dNTP-bound forms of Klentaq1 (PDB entry core 2KTQ and structure by Li *et al.* [57], respectively)]. (d) In step 3, the tip of Fingers subdomain undergoes a large conformational change resulting in the Fingers closing in onto the Palm subdomain (PDB entry code 3KTD). The closing of the Fingers subdomain brings the dNTP not only to the active site but also within Watson–Crick pairing with the templating base where the dNTP can be assessed. If the right dNTP is brought in (i.e., the dNTP making the right Watson–Crick pair with the templating base), the closed form is stabilized, leading to the reaction of the nucleotide with the 3′-OH end of the primer strand and therefore the extension of the primer by 1 nucleotide. At this stage, the cycle starts again by the binding the next dNTP in assembly (step 2).

while dNTPs are constantly brought in by the Fingers domain flapping motion and assessed for their correctness against the template base, similarly, chaperone–subunit complexes are brought to the usher by binding to the usher NTD and assessed for the correctness of their Nte's P5 residue against the P5 pocket of the previously assembled subunit. Once the correctness is assessed and the subunit/nucleotide is deemed to be "correct", the reaction occurs (DSE in one case and nucleotide incorporation in the other). DSE between FimG and FimH leads to the release of the FimH-bound chaperone and its dissociation from the CTDs, and as a result, the CTDs are now available for binding, providing the chaperone–subunit complex at the NTD the opportunity to transfer to the CTDs. This step occurs as the previously assembled subunit (FimH here) translocates through the usher pore: this step is facilitated by the ability of the CTDs to compete off the NTD-bound chaperone–subunit complex and by the helical energy path within the usher pore that imposes a rotational uplift through the pore, the extent of which is exactly what is needed to facilitate an NTD-to-CTDs transfer. Once the transfer has occurred, the usher NTD is free to recruit the next chaperone–subunit complex in assembly, and therefore, the subunit incorporation cycle resumes. Similarly, just as the building blocks for the pilus polymer (the subunits) must transfer from one binding site to another to make possible the recruitment of the next building block in assembly, the building block for the DNA (the nucleotides) must also undergo a transfer reaction: this happens in DNA Pol I when the dNTP is transferred from the Fingers subdomain to the DNA bound to the Thumb and Palm subdomains for primer extension.

Powering Pilus Biogenesis

How pilus biogenesis is powered is one of the most interesting questions in the field. There is no ATP in the bacterial periplasm and no electrochemical gradient on either side of the outer membrane; thus,

the most widespread stores of energy in biology are absent and cannot be tapped into.

Translocation during the nucleotide incorporation cycle is likely "motored" by Brownian motions. The interactions between the primer–template DNA and the polymerase are primarily electrostatic in nature. The wrapping of the protein around the DNA is thought to create an electrostatic tunnel around the DNA where interactions between the phosphoribose backbone of the DNA and charged residues on the surface of the protein are so numerous that at any moment in time, the DNA backbone can interact not only with the residues it is seen to interact with in the static crystal structures of protein–DNA complexes but also with neighboring charged residues; dynamic exchanges between interacting partners would have the effect of "lubricating" the interface, allowing the DNA to relatively freely move within the tunnel. Because the distance between stacking bases is relatively small (3–4 Å), Brownian motions would be ample enough to allow the alignment of the next template base against the active site and therefore the pairing of the next dNTP base against it (reviewed in Ref. [53]).

Brownian motions of the nascent pilus within the usher pore are also thought to be important, but because they do not impose directionality, they are just as likely to lead to the extrusion of the pilus on the outward-facing side of the usher pore or the inward-facing side of the usher pore. It could be argued that this is just as much a problem in the nucleotide incorporation cycle; Brownian motions of the DNA are as likely to go in the direction of polymerization as against. However, DNA Pol I enzymes have a particular device preventing random motions against the direction of polymerization. Indeed, DNA Pol I enzymes contain particular aromatic residues, for example, Tyr 667 in Klentaq1, against which the first unpaired base of the template (the one against which the correctness of the dNTP will be assessed) stacks; this interaction constrains Brownian motions in only one direction, that of polymerization [56,60].

In usher-mediated polymerization, the presence of such a device is unclear. It could be that a residue or a domain (perhaps the plug) acts as a ratchet, preventing the nascent pilus from random backtracking motions. Such ratcheting device could be coupled to the DSE reaction that is known to be energetically favorable [35]. However, no evidence for such a ratchet has been provided, and no structural element has yet been identified that could play such a role. Perhaps more likely, random Brownian motions drive the pilus in and out of the usher pore, but the "out" position is locked by conformational changes in the part of the nascent pilus emerging from the pore. These conformational changes able to lock the pilus in the "out" position have been particularly well documented for FimH and for the PapA rod [9,17]. The conformations of FimH pre- and post-transport are indeed known; while in a complex with FimC and bound to the usher CTDs (FimH is, at this stage, in a pre-transport conformation), the two domains of FimH are linearly aligned with respect to each other; however, as soon as FimH has entirely emerged from the usher, its lectin and pilin domains make a 37.5° angle, a conformational change large enough to prevent the nascent pilus from backtracking back into the usher pore [9]. The PapA rod structure has been recently determined and shown to be helically wound, consisting of 3.3 subunits per turn of the helix. Crucially, its diameter (81 Å) is larger than the usher pore (28 Å), and thus, once helically structured, the rod cannot backtrack within the usher pore [17]. Thus, as the rod polymer is being formed, it locks the nascent PapA polymer as it emerges out of the usher pore, thereby preventing it from backtracking within the usher pore. Thus, conformational changes and quaternary structure formation provide the energy for extrusion of the pilus. It is one of the major challenges of the field to prove that this is indeed correct.

Adhesion and Other Properties of the CU Pilus

CU pili play important roles in targeting bacterial pathogens to host tissues. Attachment of bacteria to host tissues is mediated by specific interactions between adhesins and receptors on the host cell surface.

There is a great variety of binding modes that have been observed among adhesins. To take only two examples, the adhesin PapG presents a shallow surface for binding of Galα-1,4 Gal receptors present on the kidney epithelium, and this surface is on the side of the PapG adhesin/lectin domain [24]. In contrast, FimH presents a deep binding pocket for D-mannosylated receptors on the surface of the bladder epithelium, and this pocket is at the distal tip of the FimH lectin domain [61]. In fact, the binding properties of FimH are singular, as FimH can bind its cognate receptor with either high or low affinity depending on the stretching force applied to it. More specifically, when the two domains of FimH are stretched, the mannose-binding pocket at the distal end of the lectin domain clamps shut—a mechanism likened to a "finger trap" toy [34,62,63]. In the absence of a stretching force, the linker between the two domains relaxes, and the binding affinity is low. This is thought to represent an exquisite adaptation to the natural conditions prevailing in the urinary tract; indeed, urine flow episodically generates intense shear forces, which, when a bacterium is attached to the bladder epithelium through the FimH–mannose interaction, stretches the pilus and therefore FimH, resulting in increased interaction between the bacterium and its host and thus maintaining the bacterium's foothold onto its host while the passing of urine takes place. Another remarkable adaptation to the harsh

environment of the urinary tract is the ability of the CU pilus rod to coil and uncoil depending on shear forces. Indeed, investigations of the CU pilus properties using atomic force microscopy have revealed that the pilus rod can be reversibly stretched when a force is applied [64,65]. Thus, the helical stacks of the pilus rod are able to uncoil under shear force conditions and recoil in normal conditions. This property of the pilus rod is also thought to provide the bacterium with a way to resist being flushed from the urinary tract during urine flow. The structural basis of the coiling–uncoiling transition has recently been provided by the near-atomic resolution cryo-electron microscopy structure of the P pilus rod, which revealed that interactions between helical stacks are mostly polar and weak, while the interactions mediated by DSE (between Ntes and grooves) are hydrophobic, extremely strong, and topologically essential [17]. As a result, the stacks can be disrupted easily, while the structural integrity of the polymer remains.

Conclusion

Structural, biophysical, and biochemical investigations of CU pilus biogenesis have yielded a wealth of detailed mechanistic insights that can now be exploited for practical applications. One major practical outcome of this research has been the design of inhibitors able to block specifically a number of steps in the process of polymerization and also adhesion. Bicyclic 2-pyridones, termed pilicides, have been developed to disrupt interactions between chaperone–subunit complexes and the usher NTD [66]; mannosides, mimics of mannosylated receptors, inhibit colonization and formation of intracellular biofilms and have proved to be effective in a murine infection model [67]. A new concept of pilus function disruption targets the coiling–uncoiling of pili with the hope that interfering with this process might affect the foothold of the bacterium onto host tissues [68]. The concept of designing compounds targeting virulence factors is not new but has been met with very little enthusiasm so far. Such compounds do not kill bacteria but only attenuate their virulence. However, in the case of urinary tract infections, compounds inhibiting type 1 pilus function could be particularly effective due to the singular behavior of the pathogen; indeed, upon antibiotics treatment, a small number of bacterium are able to escape their effects by forming so-called "intracellular bacterial communities", in essence biofilm sacs, which can lie asymptomatically for many months but can be reawakened to trigger another round of urinary tract infections [69]. Patients appear to be cured by the antibiotics treatment, but in fact, some bacteria have escaped treatment, and recurrence of the disease can occur without new infections at any time within weeks, months, and sometimes years. IBC formation crucially depends on type 1 pili, and thus, inhibiting type 1 pilus biogenesis would prevent IBC-mediated disease recurrence.

Acknowledgments

This work was funded by Medical Research Council grant 018434. I thank Dr. Manuela Hospenthal for comments on the manuscripts.

Received 19 April 2017;
Received in revised form 16 May 2017;
Accepted 17 May 2017
Available online 25 May 2017

Keywords:
Pilus biogenesis;
Usher;
Chaperone;
DNA polymerase I;
Nanomachine

Abbreviations used:
CU, chaperone–usher; Nte, N-terminal extension; DSE, donor-strand exchange; NTD, N-terminal domain; DNA Pol I, DNA polymerase I; dNTP, nucleoside triphosphate; DSC, donor-strand complementation.

References

[1] T.R.D. Costa, C. Felisberto-Rodrigues, A. Meir, M.S. Prevost, A. Redzej, M. Trokter, et al., Secretion systems in Gram-negative bacteria: structural and mechanistic insights, Nat. Rev. Microbiol. 13 (2015) 343–359, http://dx.doi.org/10.1038/nrmicro3456.
[2] M.M. Barnhart, M.R. Chapman, Curli biogenesis and function, Annu. Rev. Microbiol. 60 (2006) 131–147, http://dx.doi.org/10.1146/annurev.micro.60.080805.142106.
[3] G. Waksman, S.J. Hultgren, Structural biology of the chaperone–usher pathway of pilus biogenesis, Nat. Rev. Microbiol. 7 (2009) 765–774, http://dx.doi.org/10.1038/nrmicro2220.
[4] T.R.D. Costa, A. Ilangovan, M. Ukleja, A. Redzej, J.M. Santini, T.K. Smith, et al., Structure of the bacterial sex F pilus reveals an assembly of a stoichiometric protein-phospholipid complex, Cell 166 (2016) 1436–1444, http://dx.doi.org/10.1016/j.cell.2016.08.025.
[5] S. Melville, L. Craig, Type IV pili in Gram-positive bacteria, Microbiol. Mol. Biol. Rev. 77 (2013) 323–341, http://dx.doi.org/10.1128/MMBR.00063-12.
[6] H.H. Low, F. Gubellini, A. Rivera-Calzada, N. Braun, S. Connery, A. Dujeancourt, et al., Structure of a type IV secretion system, Nature 508 (2014) 550–553, http://dx.doi.org/10.1038/nature13081.
[7] Y.-W. Chang, L.A. Rettberg, A. Treuner-Lange, J. Iwasa, L. Søgaard-Andersen, G.J. Jensen, Architecture of the type IVa pilus machine, Science 351 (2016), http://dx.doi.org/10.1126/science.aad2001 First page: aad2001-1 Last page: aad2001-7.

[8] G. Phan, H. Remaut, T. Wang, W.J. Allen, K.F. Pirker, A. Lebedev, et al., Crystal structure of the FimD usher bound to its cognate FimC-FimH substrate, Nature 474 (2011) 49–53, http://dx.doi.org/10.1038/nature10109.

[9] S. Geibel, E. Procko, S.J. Hultgren, D. Baker, G. Waksman, Structural and energetic basis of folded-protein transport by the FimD usher, Nature 496 (2013) 243–246, http://dx.doi.org/10.1038/nature12007.

[10] N. Van Gerven, R.D. Klein, S.J. Hultgren, H. Remaut, Bacterial amyloid formation: structural insights into curli biogensis, Trends Microbiol. (2015) 1–14, http://dx.doi.org/10.1016/j.tim.2015.07.010.

[11] P. Goyal, P.V. Krasteva, N. Van Gerven, F. Gubellini, I. Van den Broeck, A. Troupiotis-Tsaïlaki, et al., Structural and mechanistic insights into the bacterial amyloid secretion channel CsgG, Nature 516 (2014) 250–253, http://dx.doi.org/10.1038/nature13768.

[12] G.C. Ulett, M. Totsika, K. Schaale, A.J. Carey, M.J. Sweet, M.A. Schembri, Uropathogenic *Escherichia coli* virulence and innate immune responses during urinary tract infection, Curr. Opin. Microbiol. 16 (2013) 100–107, http://dx.doi.org/10.1016/j.mib.2013.01.005.

[13] T.J. Hannan, M. Totsika, K.J. Mansfield, K.H. Moore, M.A. Schembri, S.J. Hultgren, Host-pathogen checkpoints and population bottlenecks in persistent and intracellular uropathogenic *Escherichia coli* bladder infection, FEMS Microbiol. Rev. 36 (2012) 616–648, http://dx.doi.org/10.1111/j.1574-6976.2012.00339.x.

[14] W.J. Allen, G. Phan, G. Waksman, Pilus biogenesis at the outer membrane of Gram-negative bacterial pathogens, Curr. Opin. Struct. Biol. 22 (2012) 500–506, http://dx.doi.org/10.1016/j.sbi.2012.02.001.

[15] M.J. Kuehn, J. Heuser, S. Normark, S.J. Hultgren, P pili in uropathogenic *E. coli* are composite fibres with distinct fibrillar adhesive tips, Nature 356 (1992) 252–255, http://dx.doi.org/10.1038/356252a0.

[16] E. Hahn, P. Wild, U. Hermanns, P. Sebbel, R. Glockshuber, M. Häner, et al., Exploring the 3D molecular architecture of *Escherichia coli* type 1 pili, J. Mol. Biol. 323 (2002) 845–857 http://www.ncbi.nlm.nih.gov/pubmed/12417198.

[17] M.K. Hospenthal, A. Redzej, K. Dodson, M. Ukleja, B. Frenz, C. Rodrigues, et al., Structure of a chaperone–usher pilus reveals the molecular basis of rod uncoiling, Cell 164 (2016) 269–278, http://dx.doi.org/10.1016/j.cell.2015.11.049.

[18] B. Lund, F. Lindberg, B.I. Marklund, S. Normark, The PapG protein is the alpha-D-galactopyranosyl-(1-4)-beta-D-galactopyranose-binding adhesin of uropathogenic *Escherichia coli*, Proc. Natl. Acad. Sci. U. S. A. 84 (1987) 5898–5902.

[19] F. Lindberg, B. Lund, L. Johansson, S. Normark, Localization of the receptor-binding protein adhesin at the tip of the bacterial pilus, Nature 328 (1987) 84–87, http://dx.doi.org/10.1038/328084a0.

[20] M.A. Mulvey, Adhesion and entry of uropathogenic *Escherichia coli*, Cell. Microbiol. 4 (2002) 257–271 http://www.ncbi.nlm.nih.gov/pubmed/12027955.

[21] S.N. Abraham, D. Sun, J.B. Dale, E.H. Beachey, Conservation of the D-mannose-adhesion protein among type 1 fimbriated members of the family, Enterobacteriaceae 336 (1988) 682–684, http://dx.doi.org/10.1038/336682a0.

[22] F.G. Sauer, K. Fütterer, J.S. Pinkner, K.W. Dodson, S.J. Hultgren, G. Waksman, Structural basis of chaperone function and pilus biogenesis, Science 285 (1999) 1058–1061.

[23] D. Choudhury, A. Thompson, V. Stojanoff, S. Langermann, J. Pinkner, S.J. Hultgren, et al., X-ray structure of the FimC-FimH chaperone-adhesin complex from uropathogenic *Escherichia coli*, Science 285 (1999) 1061–1066 http://www.ncbi.nlm.nih.gov/pubmed/10446051.

[24] K.W. Dodson, J.S. Pinkner, T. Rose, G. Magnusson, S.J. Hultgren, G. Waksman, Structural basis of the interaction of the pyelonephritic *E. coli* adhesin to its human kidney receptor, Cell 105 (2001) 733–743 http://www.ncbi.nlm.nih.gov/pubmed/11440716.

[25] M.M. Barnhart, J.S. Pinkner, G.E. Soto, F.G. Sauer, S. Langermann, G. Waksman, et al., PapD-like chaperones provide the missing information for folding of pilin proteins, Proc. Natl. Acad. Sci. 97 (2000) 7709–7714, http://dx.doi.org/10.1073/pnas.130183897.

[26] M. Vetsch, C. Puorger, T. Spirig, U. Grauschopf, E.U. Weber-Ban, R. Glockshuber, Pilus chaperones represent a new type of protein-folding catalyst, Nature 431 (2004) 329–332, http://dx.doi.org/10.1038/nature02834.

[27] A. Holmgren, C.I. Bränden, Crystal structure of chaperone protein PapD reveals an immunoglobulin fold, Nature 342 (1989) 248–251, http://dx.doi.org/10.1038/342248a0.

[28] M.J. Kuehn, D.J. Ogg, J. Kihlberg, L.N. Slonim, K. Flemmer, T. Bergfors, et al., Structural basis of pilus subunit recognition by the PapD chaperone, Science 262 (1993) 1234–1241.

[29] G.E. Soto, K.W. Dodson, D. Ogg, C. Liu, J. Heuser, S. Knight, et al., Periplasmic chaperone recognition motif of subunits mediates quaternary interactions in the pilus, EMBO J. 17 (1998) 6155–6167, http://dx.doi.org/10.1093/emboj/17.21.6155.

[30] F.G. Sauer, J.S. Pinkner, G. Waksman, S.J. Hultgren, Chaperone priming of pilus subunits facilitates a topological transition that drives Fiber formation, Cell 111 (2002) 543–551.

[31] H. Remaut, R.J. Rose, T.J. Hannan, S.J. Hultgren, S.E. Radford, A.E. Ashcroft, et al., Donor-strand exchange in chaperone-assisted pilus assembly proceeds through a concerted beta strand displacement mechanism, Mol. Cell 22 (2006) 831–842, http://dx.doi.org/10.1016/j.molcel.2006.05.033.

[32] A.V. Zavialov, J. Berglund, A.F. Pudney, L.J. Fooks, T.M. Ibrahim, S. MacIntyre, et al., Structure and biogenesis of the capsular F1 antigen from *Yersinia pestis*: preserved folding energy drives Fiber formation, Cell 113 (2003) 587–596.

[33] D. Verger, E. Bullitt, S.J. Hultgren, G. Waksman, Crystal structure of the P pilus rod subunit PapA, PLoS Pathog. 3 (2007) e73, http://dx.doi.org/10.1371/journal.ppat.0030073.

[34] I. Le Trong, P. Aprikian, B.A. Kidd, M. Forero-Shelton, V. Tchesnokova, P. Rajagopal, et al., Structural basis for mechanical force regulation of the adhesin FimH via finger trap-like sheet twisting, Cell 141 (2010) 645–655, http://dx.doi.org/10.1016/j.cell.2010.03.038.

[35] C. Puorger, O. Eidam, G. Capitani, D. Erilov, M.G. Grütter, R. Glockshuber, Infinite kinetic stability against dissociation of supramolecular protein complexes through donor strand complementation, Structure 16 (2008) 631–642, http://dx.doi.org/10.1016/j.str.2008.01.013.

[36] C. Puorger, M. Vetsch, G. Wider, R. Glockshuber, Structure, folding and stability of FimA, the main structural subunit of type 1 pili from uropathogenic *Escherichia coli* strains, J. Mol. Biol. 412 (2011) 520–535, http://dx.doi.org/10.1016/j.jmb.2011.07.044.

[37] R.J. Rose, T.S. Welsh, G. Waksman, A.E. Ashcroft, S.E. Radford, E. Paci, Donor-strand exchange in chaperone-assisted pilus assembly revealed in atomic detail by molecular dynamics, J. Mol. Biol. 375 (2008) 908–919, http://dx.doi.org/10.1016/j.jmb.2007.10.077.

[38] R.J. Rose, D. Verger, T. Daviter, H. Remaut, E. Paci, G. Waksman, et al., Unraveling the molecular basis of subunit

specificity in P pilus assembly by mass spectrometry, Proc. Natl. Acad. Sci. U. S. A. 105 (2008) 12,873–12,878, http://dx.doi.org/10.1073/pnas.0802177105.
[39] A.C. Leney, G. Phan, W. Allen, D. Verger, G. Waksman, S.E. Radford, et al., Second order rate constants of donor-strand exchange reveal individual amino acid residues important in determining the subunit specificity of pilus biogenesis, J. Am. Soc. Mass Spectrom. 22 (2011) 1214–1223, http://dx.doi.org/10.1007/s13361-011-0146-4.
[40] D. Verger, E. Miller, H. Remaut, G. Waksman, S. Hultgren, Molecular mechanism of P pilus termination in uropathogenic *Escherichia coli*, EMBO Rep. 7 (2006) 1228–1232, http://dx.doi.org/10.1038/sj.embor.7400833.
[41] K.W. Dodson, F. Jacob-Dubuisson, R.T. Striker, S.J. Hultgren, Outer-membrane PapC molecular usher discriminately recognizes periplasmic chaperone-pilus subunit complexes, Proc. Natl. Acad. Sci. 90 (1993) 3670–3674.
[42] E.T. Saulino, D.G. Thanassi, J.S. Pinkner, S.J. Hultgren, Ramifications of kinetic partitioning on usher-mediated pilus biogenesis, EMBO J. 17 (1998) 2177–2185, http://dx.doi.org/10.1093/emboj/17.8.2177.
[43] M. Nishiyama, T. Ishikawa, H. Rechsteiner, R. Glockshuber, Reconstitution of pilus assembly reveals a bacterial outer membrane catalyst, Science 320 (2008) 376–379, http://dx.doi.org/10.1126/science.1154994.
[44] W.J. Allen, G. Phan, S.J. Hultgren, G. Waksman, Dissection of pilus tip assembly by the FimD usher monomer, J. Mol. Biol. 425 (2013) 958–967, http://dx.doi.org/10.1016/j.jmb.2012.12.024.
[45] M. Nishiyama, M. Vetsch, C. Puorger, I. Jelesarov, R. Glockshuber, Identification and characterization of the chaperone–subunit complex-binding domain from the type 1 pilus assembly platform FimD, J. Mol. Biol. 330 (2003) 513–525.
[46] T.W. Ng, L. Akman, M. Osisami, D.G. Thanassi, The usher N terminus is the initial targeting site for chaperone–subunit complexes and participates in subsequent pilus biogenesis events, J. Bacteriol. 186 (2004) 5321–5331, http://dx.doi.org/10.1128/JB.186.16.5321-5331.2004.
[47] N.S. Henderson, T.W. Ng, I. Talukder, D.G. Thanassi, Function of the usher N-terminus in catalysing pilus assembly, Mol. Microbiol. 79 (2010) 954–967, http://dx.doi.org/10.1111/j.1365-2958.2010.07505.x.
[48] B. Morrissey, A.C. Leney, A. Toste Rêgo, G. Phan, W.J. Allen, D. Verger, et al., The role of chaperone–subunit usher domain interactions in the mechanism of bacterial pilus biogenesis revealed by ESI-MS, Mol. Cell. Proteomics 11 (7) (2012) M111.015289 http://dx.doi.org/10.1074/mcp.M111.015289 Epub 2012 Feb 27.
[49] E. Volkan, B.A. Ford, J.S. Pinkner, K.W. Dodson, N.S. Henderson, D.G. Thanassi, et al., Domain activities of PapC usher reveal the mechanism of action of an *Escherichia coli* molecular machine, Proc. Natl. Acad. Sci. U. S. A. 109 (2012) 9563–9568, http://dx.doi.org/10.1073/pnas.1207085109.
[50] H. Remaut, C. Tang, N.S. Henderson, J.S. Pinkner, T. Wang, S.J. Hultgren, et al., Fiber formation across the bacterial outer membrane by the chaperone/usher pathway, Cell 133 (2008) 640–652, http://dx.doi.org/10.1016/j.cell.2008.03.033.
[51] T. Pham, G.T. Werneburg, N.S. Henderson, D.G. Thanassi, A.H. Delcour, Effect of chaperone-adhesin complex on plug release by the PapC usher, FEBS Lett. 590 (2016) 2172–2179, http://dx.doi.org/10.1002/1873-3468.12257.
[52] O.S. Mapingire, N.S. Henderson, G. Duret, D.G. Thanassi, A.H. Delcour, Modulating effects of the plug, helix, and N- and C-terminal domains on channel properties of the PapC usher, J. Biol. Chem. 284 (2009) 36,324–36,333, http://dx.doi.org/10.1074/jbc.M109.055798.
[53] P.J. Rothwell, G. Waksman, Structure and mechanism of DNA polymerases, Adv. Protein Chem. (2005) 401–440, http://dx.doi.org/10.1016/S0065–3233(04)71011-6.
[54] S. Doublié, M.R. Sawaya, T. Ellenberger, An open and closed case for all polymerases, Structure/Folding and Design 7 (1999) R31–R35, http://dx.doi.org/10.1016/S0969-2126(99)80017-3.
[55] S. Korolev, M. Nayal, W.M. Barnes, E. Di Cera, G. Waksman, Crystal structure of the large fragment of *Thermus aquaticus* DNA polymerase I at 2.5-A resolution: structural basis for thermostability, Proc. Natl. Acad. Sci. 92 (1995) 9264–9268.
[56] Y. Li, S. Korolev, G. Waksman, Crystal structures of open and closed forms of binary and ternary complexes of the large fragment of *Thermus aquaticus* DNA polymerase I: structural basis for nucleotide incorporation, EMBO J. 17 (1998) 7514–7525, http://dx.doi.org/10.1093/emboj/17.24.7514.
[57] Y. Li, Y. Kong, S. Korolev, G. Waksman, Crystal structures of the Klenow fragment of *Thermus aquaticus* DNA polymerase I complexed with deoxyribonucleoside triphosphates, Protein Sci. 7 (1998) 1116–1123, http://dx.doi.org/10.1002/pro.5560070505.
[58] P.J. Rothwell, W.J. Allen, E. Sisamakis, S. Kalinin, S. Felekyan, J. Widengren, et al., dNTP-dependent conformational transitions in the fingers subdomain of Klentaq1 DNA polymerase: insights into the role of the "nucleotide-binding" state, J. Biol. Chem. 288 (2013) 13,575–13,591, http://dx.doi.org/10.1074/jbc.M112.432690.
[59] P.J. Rothwell, V. Mitaksov, G. Waksman, Motions of the fingers subdomain of Klentaq1 are fast and not rate limiting: implications for the molecular basis of fidelity in DNA polymerases, Mol. Cell 19 (2005) 345–355, http://dx.doi.org/10.1016/j.molcel.2005.06.032.
[60] S. Doublié, S. Tabor, A.M. Long, C.C. Richardson, T. Ellenberger, Crystal structure of a bacteriophage T7 DNA replication complex at 2.2 A resolution, Nature 391 (1998) 251–258, http://dx.doi.org/10.1038/34593.
[61] C.S. Hung, J. Bouckaert, D. Hung, J. Pinkner, C. Widberg, A. DeFusco, et al., Structural basis of tropism of *Escherichia coli* to the bladder during urinary tract infection, Mol. Microbiol. 44 (2002) 903–915.
[62] P. Aprikian, G. Interlandi, B.A. Kidd, I. Le Trong, V. Tchesnokova, O. Yakovenko, et al., The bacterial fimbrial tip acts as a mechanical force sensor, PLoS Biol. 9 (2011) e1000617, http://dx.doi.org/10.1371/journal.pbio.1000617.
[63] P. Aprikian, V. Tchesnokova, B. Kidd, O. Yakovenko, V. Yarov-Yarovoy, E. Trinchina, et al., Interdomain interaction in the FimH adhesin of *Escherichia coli* regulates the affinity to mannose, J. Biol. Chem. 282 (2007) 23,437–23,446, http://dx.doi.org/10.1074/jbc.M702037200.
[64] E. Fällman, S. Schedin, J. Jass, B.E. Uhlin, O. Axner, The unfolding of the P pili quaternary structure by stretching is reversible, not plastic, EMBO Rep. 6 (2005) 52–56, http://dx.doi.org/10.1038/sj.embor.7400310.
[65] M. Forero, O. Yakovenko, E.V. Sokurenko, W.E. Thomas, V. Vogel, Uncoiling mechanics of *Escherichia coli* type I fimbriae are optimized for catch bonds, PLoS Biol. 4 (2006) e298, http://dx.doi.org/10.1371/journal.pbio.0040298.
[66] E. Chorell, J.S. Pinkner, G. Phan, S. Edvinsson, F. Buelens, H. Remaut, et al., Design and synthesis of C-2 substituted thiazolo and dihydrothiazolo ring-fused 2-pyridones: pilicides with increased antivirulence activity, J. Med. Chem. 53 (2010) 5690–5695, http://dx.doi.org/10.1021/jm100470t.
[67] C.K. Cusumano, J.S. Pinkner, Z. Han, S.E. Greene, B.A. Ford, J.R. Crowley, et al., Treatment and prevention of urinary tract

infection with orally active FimH inhibitors, Sci. Transl. Med. 3 (2011) http://dx.doi.org/10.1126/scitranslmed.3003021 First page :109ra115 Last page: 109ra115.

[68] J.E. Klinth, J.S. Pinkner, S.J. Hultgren, F. Almqvist, B.E. Uhlin, O. Axner, Impairment of the biomechanical compliance of P pili: a novel means of inhibiting uropathogenic bacterial infections? Eur. Biophys. J. 41 (2012) 285–295, http://dx.doi.org/10.1007/s00249-011-0784-2.

[69] G.G. Anderson, J.J. Palermo, J.D. Schilling, R. Roth, J. Heuser, S.J. Hultgren, Intracellular bacterial biofilm-like pods in urinary tract infections, Science 301 (2003) 105–107, http://dx.doi.org/10.1126/science.1084550.

[70] G.T. Werneburg, N.S. Henderson, E.B. Portnoy, S. Sarowar, S.J. Hultgren, H. Li, D.G. Thanassi, The pilus usher controls protein interactions via domain masking and is functional as an oligomer, Nat. Struct. Mol. Biol. 22 (2015) 540–546, http://dx.doi.org/10.1038/nsmb.3044.